noise, and a deconvolution filter was applied to attenuate multiples and improve the quality of reflections. The data files were then exported figures were created.

Processed GPR cross sections are shown throughout this chapter. The sections are displayed with the horizontal (length) and vertical (depth) scales in ft and m using a velocity calculated with the dielectric constant, ε_r, equal to 8. Note the slight exaggeration in the vertical scale. The sections are displayed in a line scan format using a grayscale palette. Interpreted figures, shown in this section, are provided with known caves highlighted in blue, and suspected caves highlighted in red. Uninterrupted GPR figures are included in appendix C. The 200 MHz data, rather than the 400 MHz data, has been selected for interpretation because it provides a greater depth of penetration although resolution is less than that which can be obtained with the 400 MHz data. In addition, because the 200 MHz antenna provides a longer wavelength than the 400 MHz antenna, the signal is less susceptible to scattering.

The descriptions of the GPR data acquisition, processing, and interpretation procedures apply to all of the cave sites in this report.

To maximize coverage at Golden Dome Cave, three profiles were collected at different angles and different lengths with each of the GPR antennae. Figure 17 shows the approximate location of the survey lines superimposed on a plan map obtained from The Lava Beds Caves book. It appears that the survey lines cross the cave; however, after surveying with a compass and chain, it was determined that the cave is actually further west than is shown in the figure. Therefore, the GPR survey was not conducted over the cave. Table 4 gives the coordinates of the start and end point of each GPR line at this site.

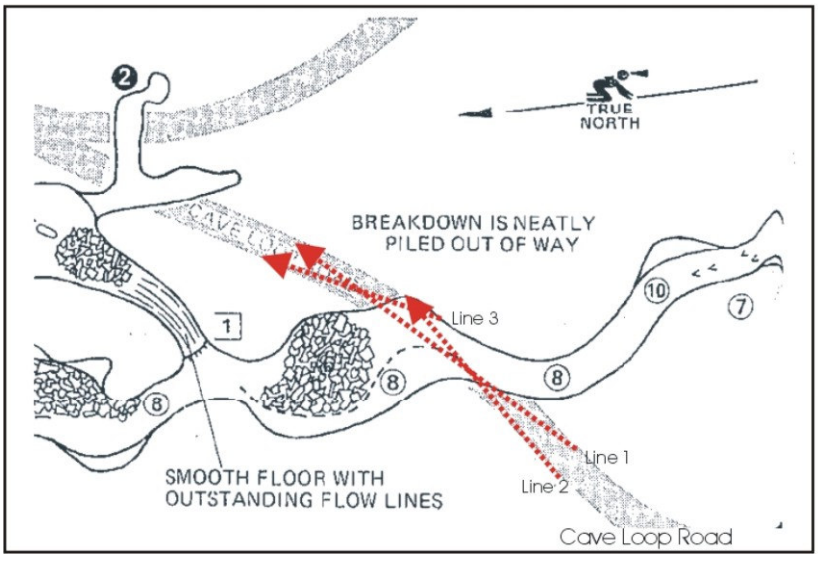

Figure 17. Map. GPR survey lines over Golden Dome Cave. [6]

Table 4. GPR survey line coordinates over Golden Dome Cave.

Line #	Southwest End Point		Northeast End Point	
	Easting (m)	Northing (m)	Easting (m)	Northing (m)
Line 1	623654.38	4618750.3	623685.26	4618788.08
Line 2	623654.45	4618750.33	623676.13	4618767.79
Line 3	623672.37	4618762.61	623681.54	4618788.15
All coordinates are listed in NAD 83/UTM Zone 10				

Figure 18 displays the 200 MHz antenna data collected at the Golden Dome Cave survey site. Since GPR data were not collected over the known cave, the known cave is not outlined on the GPR cross section. All measurements discussed are from the start of the profile (0 m), unless otherwise noted. Multiple anomalies (hyperbolae) are visible in the first 10.7 m (35.1 ft) of the profile. Of these, three have been outlined in red as possible lava tubes. Two of the hyperbolae are centered at 7.6 m (24.9 ft), and almost completely overlap, although they are interpreted to lie at different depths, 3.4 m and 2.1 m (11.2 ft and 6.9 ft), and have slightly different widths, 4.9 m and 5.8 m (16.1 ft and 19 ft), respectively. Widths of GPR anomalies are estimates based on analysis of the width of the diffraction hyperbolas. The third hyperbola is centered at 9.8 m (32.2 ft) at a depth of 2.7 m (8.9 ft) with a width of 4.3 m (14.1 ft). These anomalies are small and may represent very small lava tubes, blisters, or fracturing in the rock. Two high amplitude anomalies are outlined in the data as well. A small hyperbola is visible at 31.7 m (104.0 ft). It is characterized by a high amplitude response at its apex and along the right tail while the left tail is lost in an area of multiple diffractions. The last area outlined, between 38.1 and 48.8 m (125.0 and 160.1 ft), is comprised of a possible layer as well as a high amplitude hyperbola. The hyperbola is less than 3.0 m (9.8 ft) in width but has a very high amplitude response. These anomalies may be caused by small lava tubes, blisters, or fracturing.

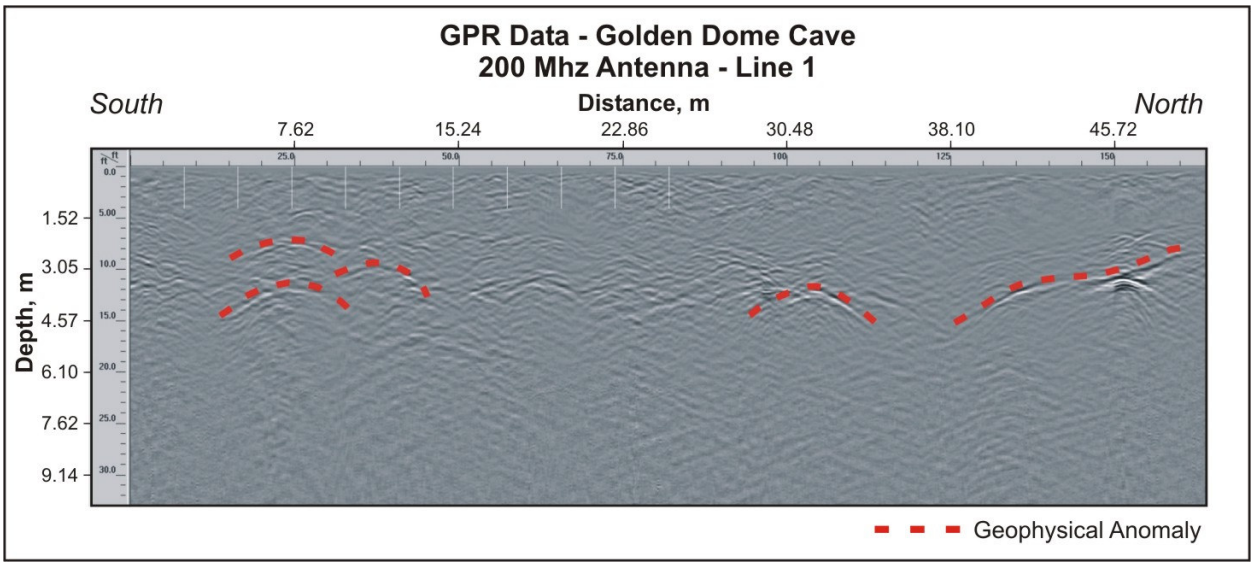

Figure 18. Profile. GPR cross section collected over Golden Dome Cave.

Magnetic Method

Three lines of magnetic data were collected along the road section at each site. One line was collected down either side of the road and one line was collected in the middle of the road. The line spacing was between 1.5 and 2.2 m (4.9 and 7.2 ft). The magnetic data was collected with a Geometrics G-858 magnetometer, which measures the magnitude of the magnetic field vector, at a rate of 10 measurements per second. The data were coupled with DGPS for positioning. A base station magnetometer was recorded during the magnetic survey.

The magnetic data was processed in MagMap2000. In this program, data files were inspected for data spikes, a diurnal correction was applied to the data, DGPS antenna offset corrections were applied, the diurnal magnetic field was removed, and the data were exported with spatial coordinates associated with each magnetic field data point (*.xyz ASCII format). The ASCII files were then read into Oasis montaj where the data from each line were shifted slightly to compensate for spatial errors in the GPS data and figures were created.

The descriptions of the magnetic data acquisition, processing, and interpretation procedures apply to all of the cave sites in this report.

Figure 19 shows the magnetic data collected over Golden Dome Cave. The top of the figure shows gridded data from all three lines along the road. The bottom of the figure shows magnetic profiles from all three survey lines. The direction of the magnetic profile is SW-NE.

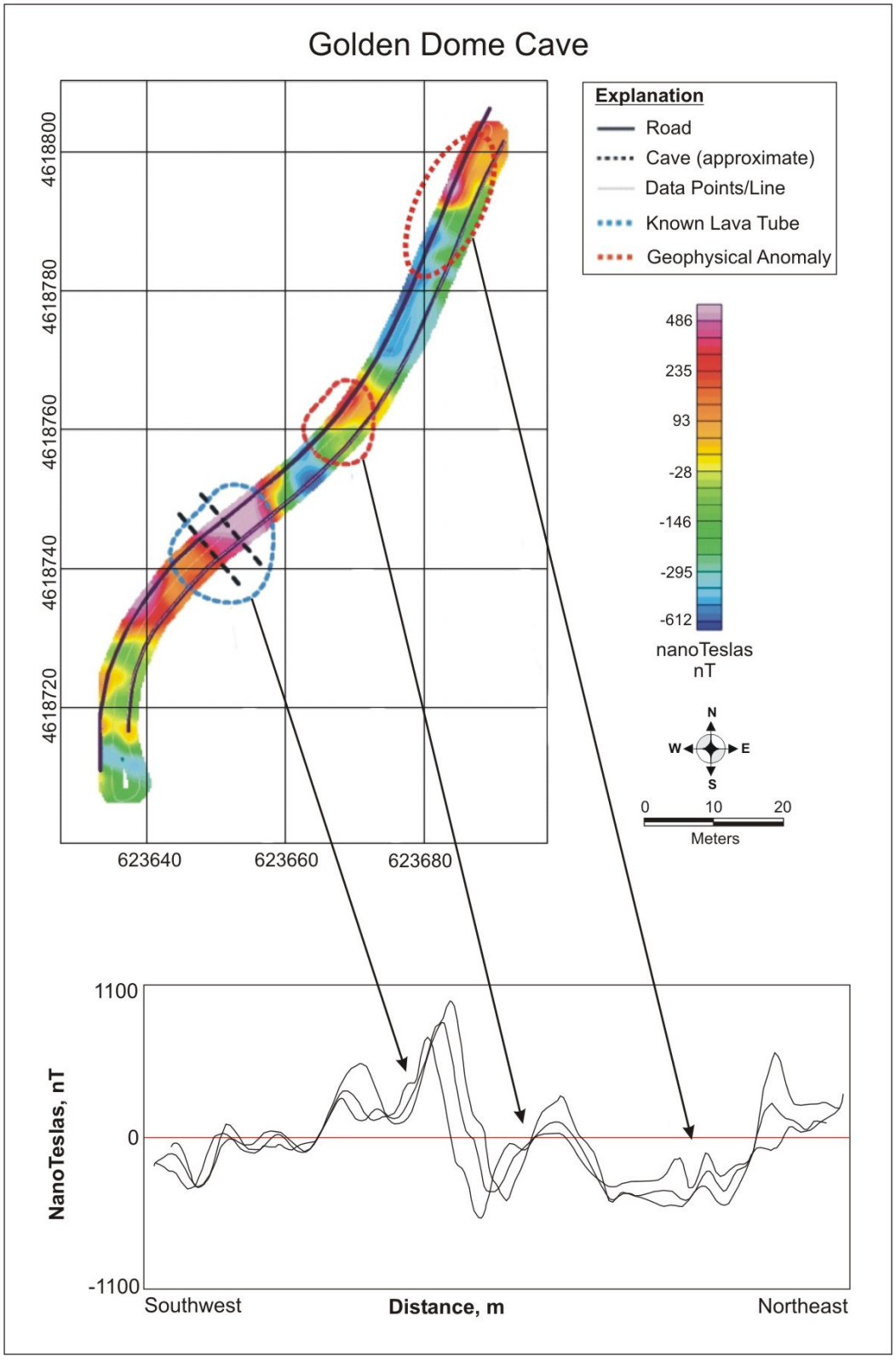

Figure 19. Map. Plan and profile view of magnetic data collected over Golden Dome Cave

The interpretation of magnetic anomalies for lava tubes in this environment is quite challenging. The feature of interest is a void, and is therefore a non-magnetic source. This contrasts with the usual magnetic anomaly interpretations where magnetic sources are interpreted. In addition, it is possible that remnant magnetization exists whose direction is different from that of any induced magnetization. The basalts and other rocks may have different concentrations of magnetite in different locations, thus forming anomalies unrelated to voids. However, a simple visual analysis of the type of anomaly that can be expected over a void suggests that if the anomaly results from induced magnetization alone then a bipolar anomaly should be seen with the negative part of the anomaly occurring to the south of the void and the positive part to the north. However, it should be kept in mind that this simple shape may be significantly modified if the factors described above become prominent.

The response of the void in magnetic data will vary from site to site. Magnetic data interpretation requires information on the site's location, including the inclination and declination of the survey, the geologic conditions, and the survey's orientation. Because of the large number of factors that may be involved in the production of anomalies, it is not possible in this report to ascribe a physical explanation to every anomaly. Thus, for each of the sites where magnetic data were acquired, only a brief discussion is provided, mostly pointing out the anomalies and their association with known caves, or their potential to indicate unknown caves.

Figure 19 shows that the largest anomaly correlates well, spatially, with the known cave location. The survey width of the cave is approximately 3.8 m (12.5 ft) and the surveyed depth to its top is 4.0 m (13.1 ft). Two other anomalies located northeast of the known cave were selected as a possible cave location along the survey lines. Both anomalies have characteristics similar to the anomaly over the lava tube. It may be possible to model these anomalies using computer software, possibly providing more details about the geometry of the lava tube. Although brief attempts at modeling have been made, much more analysis needs to be done and no conclusions are currently drawn from the modeling.

Seismic Reflection

High Resolution Shear Wave reflection data were collected along 57.9 m (190 ft) profiles at most sites (a longer profile line was collected at Hercules Leg). The Land Streamer consists of 96 geophones at 0.61 m (2 ft) intervals. The first geophone on the Land Streamer was designated as geophone 101 and the last geophone as 196. The MicroVibrator was positioned adjacent to the Land Streamer and between two geophones, called half stations. Data collection began at shot point 101.5 and continued through shot point 195.5. Data acquisition parameters are included in appendix B.

The S-wave data were processed using the UNIX-based ProMax® software. The processing flow is based on a standard common midpoint (CMP) reflection processing sequence with modification for specific conditions at the survey site. Each line was processed individually while all area-based parameters were kept constant.